Decoupled crust-mantle accommodation of Africa-Eurasia convergence in the NW Moroccan margin

I. Jiménez-Munt,[1] M. Fernàndez,[1] J. Vergés,[1] D. Garcia-Castellanos,[1] J. Fullea,[2] M. Pérez-Gussinyé,[3] and J. C. Afonso[4]

Received 15 November 2010; revised 26 May 2011; accepted 6 June 2011; published 16 August 2011.

[1] The extent of the area accommodating convergence between the African and Iberian plates, how this convergence is partitioned between crust and mantle, and the role of the plate boundary in accommodating deformation are not well-understood subjects. We calculate the structure of the lithosphere derived from its density distribution along a profile running from the Tagus Abyssal Plain to the Sahara Platform and crossing the Gorringe Bank, the NW Moroccan margin, and the Atlas Mountains. The model is based on the integration of gravity, geoid, elevation, and heat flow data and on the crustal structure across the NW Moroccan margin derived from reflection and wide-angle seismic data. The resulting mantle density anomalies suggest important variations of the lithosphere-asthenosphere boundary (LAB) topography, indicating prominent lithospheric mantle thickening beneath the margin (LAB > 200 km depth) followed by thinning beneath the Atlas Mountains (LAB ~90 km depth). At crustal levels the Iberia-Africa convergence is sparsely accommodated in a ~950 km wide area and localized in the Atlas and Gorringe regions, with an inferred shortening of ~50 km. In contrast, mantle thickening accommodates a 400 km wide region, thus advocating for a decoupled crustal-mantle mechanical response. A combination of mantle underthrusting due to oblique convergence, together with a viscous dripping fed by lateral mantle dragging, can explain the imaged lithospheric structure. The model is consistent with crustal shortening estimates and with the accommodation of part of the Iberia-Africa convergence farther NW of the Gorringe Bank and/or off the strike of the profile.

Citation: Jiménez-Munt, I., M. Fernàndez, J. Vergés, D. Garcia-Castellanos, J. Fullea, M. Pérez-Gussinyé, and J. C. Afonso (2011), Decoupled crust-mantle accommodation of Africa-Eurasia convergence in the NW Moroccan margin, *J. Geophys. Res.*, *116*, B08403, doi:10.1029/2010JB008105.

1. Introduction

[2] The African-Eurasian plate boundary between the Azores triple junction and the Gibraltar Strait is characterized by a complex tectonic regime, varying from transtensive in the west to transpressive in the east, with strike-slip motion in its central segment (Figure 1). Seismic data and numerical modeling reveal that the plate boundary is relatively narrow to the west of the Gorringe Bank, whereas deformation spreads over a much broader region to the east toward the Betic-Rif orogen and the inner Alboran Basin [*Buforn et al.*, 1988; *Jiménez-Munt et al.*, 2001]. The convergence rate between the African and European plates on the NW Moroccan margin is ~3.5 mm yr^{-1} in a WNW direction, predicted from paleomagnetic field measurements and slip vectors [*Argus et al.*, 1989], from numerical models [*Jiménez-Munt and Negredo*, 2003] and from GPS data [e.g., *Calais et al.*, 2003; *Nocquet and Calais*, 2004; *Fernandes et al.*, 2007]. How this convergence is distributed between the two plate margins is a matter of active debate.

[3] Global and regional tomography shows a clear fast velocity zone affecting the western Betics and Rif in the first hundred kilometers, which dips to the east, reaching the 410 km discontinuity [*Bijwaard and Spakman*, 2000; *Calvert et al.*, 2000]. This anomaly seems to extend further to the SW along the Moroccan margin although the poor ray coverage in this region prevents for firm conclusions. NW-SE lithospheric profiles combining geopotential, lithostatic, and thermal analyses imaged a prominent lithospheric thinning across the Atlas Mountains and an incipient lithospheric thickening beneath the NW Moroccan continental margin [*Zeyen et al.*, 2005; *Teixell et al.*, 2005; *Missenard et al.*, 2006]. One-dimensional joint inversion of elevation and geoid anomaly data predicted an elongated lithospheric thickening along the NW Moroccan margin from the Gibraltar Arc to the 33°N parallel [*Fullea et al.*, 2007]. This thickening is also supported by a recent study based on a 3-D integrated geophysical-

[1]Group of Dynamics of the Lithosphere, Institute of Earth Sciences Jaume Almera, CSIC, Barcelona, Spain.
[2]Dublin Institute for Advanced Studies, Dublin, Ireland.
[3]Department of Earth Sciences, Royal Holloway University of London, Egham, UK.
[4]GEMOC ARC National Key Centre, Macquarie University, Sydney, New South Wales, Australia.

0148-0227/11/2010JB008105

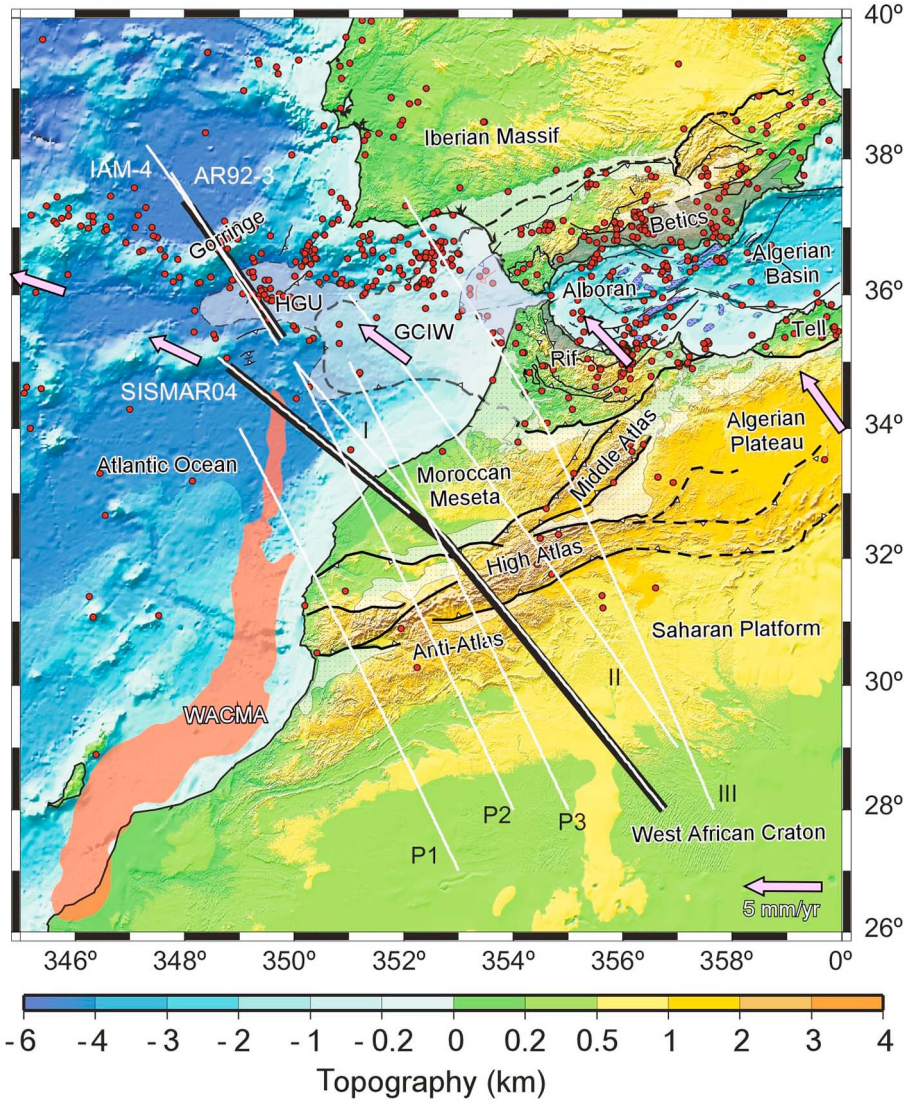

Figure 1. Elevation and earthquakes distribution from IGN with magnitude >4. IAM-4, AR92-3 and SISMAR04 correspond to the position of seismic surveys of *Banda et al.* [1995], *Sartori et al.* [1994], and *Contrucci et al.* [2004], respectively. Other profiles correspond to integrated lithosphere models of the Atlas Mountains: I, II, and III [*Teixell et al.*, 2005; *Zeyen et al.*, 2005] and P1, P2, and P3 [*Missenard et al.*, 2006]. The thick black line is the position of our profile. Arrows show the relative motion between Africa and Eurasia. HGU, horseshoe gravitational unit; GCIW, Gulf of Cadiz imbricate wedge; WACMA, West African coast magnetic anomaly.

petrological model [*Fullea et al.*, 2010]. A common caveat of the aforementioned models is the relative lack of resolution on the crustal structure across the NW Moroccan margin, which might lead to uncertainties in the estimation of the lithospheric thickness. The completion of the SISMAR deep seismic survey offshore Morocco [e.g., *Contrucci et al.*, 2004] brings a superb opportunity to constrain the structure of the crust and the uppermost mantle and hence to get a more reliable image of the geometry of the lithosphere-asthenosphere boundary (LAB) beneath the NW Moroccan margin.

[4] The aims of this work are (1) to analyze the lithosphere structure of the NW Moroccan margin by incorporating recent wide-angle and reflection seismic data across the margin [*Contrucci et al.*, 2004] and (2) to study how deformation related to the Africa-Eurasia convergence is accommodated beyond the plate boundary over a region including the Gorringe Bank, the Moroccan margin, and the Atlas Mountains as major tectonic structures. To this end we use a 2-D numerical approach that solves simultaneously the geopotential, lithostatic and heat transport equations in steady state [e.g., *Zeyen and Fernàndez*, 1994; *Zeyen et al.*, 2005] and regional isostasy [*Jiménez-Munt et al.*, 2010]. The NW segment of the modeled lithospheric profile crosses the Gorringe Bank and has been the subject of a recent study by *Jiménez-Munt et al.* [2010] using the same methodology.

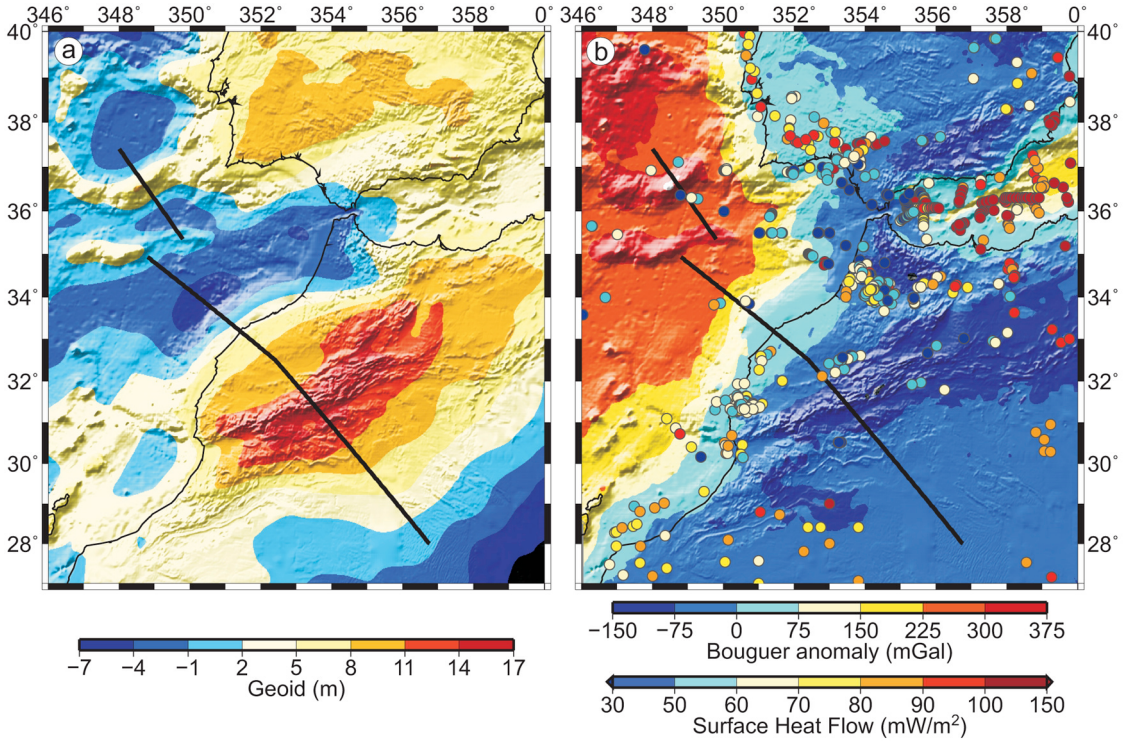

Figure 2. (a) Geoid high anomaly taken from EGM2008 and filtered for spherical harmonics up to degree and order of 9. (b) Bouguer gravity anomaly map in colors and measured surface heat flow in circles. Shades are the elevation data, and the thick black line is the position of the profile.

The central segment coincides with the seismic survey SISMAR04 [*Contrucci et al.*, 2004; *Jaffal et al.*, 2009], which crosses the Moroccan margin from SE of Coral Patch to the shoreline. The SE segment continues inland along profile 1 modeled by *Teixell et al.* [2005]. The profile ends in the Sahara craton with a total length of 1360 km (thick black lines in Figure 1).

2. Regional Data

[5] Elevation, geoid and gravity anomaly, and heat flow data of the region are shown in Figures 1 and 2. Elevation data obtained from GINA Global Topo Data [*Lindquist et al.*, 2004] show prominent topographic features such as the high of the Gorringe Bank seamount, the steep Moroccan margin, and the elevated topography in the Atlas Mountains (Figure 1). Geoid height (Figure 2a) is taken from the recent EGM2008 global model [*Pavlis et al.*, 2008]. In order to avoid effects of sublithospheric density variations on the geoid, we have removed the geoid signature corresponding to the lower spherical harmonics until degree and order 9. The obtained geoid anomaly shows an amplitude exceeding 22 m with a maximum of 16 m in the Atlas Mountains and a minimum of −6 m beside the continental slope. This minimum tends to vanish southwestward perpendicularly to the profile. The Bouguer gravity anomaly (Figure 2b) comes from *Hildenbrand et al.* [1988] onshore Morocco, while for the rest of the African region and offshore regions the Bouguer anomaly is calculated applying the complete Bouguer correction to free air satellite data [*Sandwell and Smith*, 1997] using the software FA2BOUG [*Fullea et al.*, 2008]. The Bouguer anomaly shows a marked maximum of ~380 mGal in the Gorringe Bank decreasing to the SE across the margin until a minimum value of ~−120 mGal in the Atlas Mountains. The Sahara Platform shows rather constant values around −40 mGal. Surface heat flow measurements in the area come from different studies [*Verzhbitsky and Zolotarev*, 1989; *Polyak et al.*, 1996; *Fernàndez et al.*, 1998; *Rimi et al.*, 1998; *Grevemeyer et al.*, 2009] (Figure 2b). The heat flow data present a wide scatter with average values of ~50 mW m^{-2} in the oceanic domain and more than 65 mW m^{-2} in the continental domain, values which might be affected by groundwater flow and hydrothermal activity [*Rimi et al.*, 1998].

3. Crustal Structure

[6] The crustal structure in the Gorringe Bank segment (between 0 and 270 km in horizontal distance; see Figure 3e) has been taken from seismic profiles IAM-4 [*Banda et al.*, 1995] and AR92-3 [*Sartori et al.*, 1994] and from the recent interpretation based on integrated geophysical modeling presented by *Jiménez-Munt et al.* [2010]. Across the central segment of the transect (between 270 and 580 km in horizontal distance; see Figures 3e and 4) the crustal structure comes from the interpretation of the SISMAR04 seismic survey by *Contrucci et al.* [2004]. According to Contrucci et al., the crust-mantle boundary lies at 35 km depth around the shoreline shallowing seaward to 15–17 km depth in the Seine Abyssal Plain. A 6 km thick sedimentary basin along the foot of the slope characterizes the shallow structure of the margin. The geometries and densities of sedimentary and crustal layers have been taken from *Contrucci et al.* [2004],

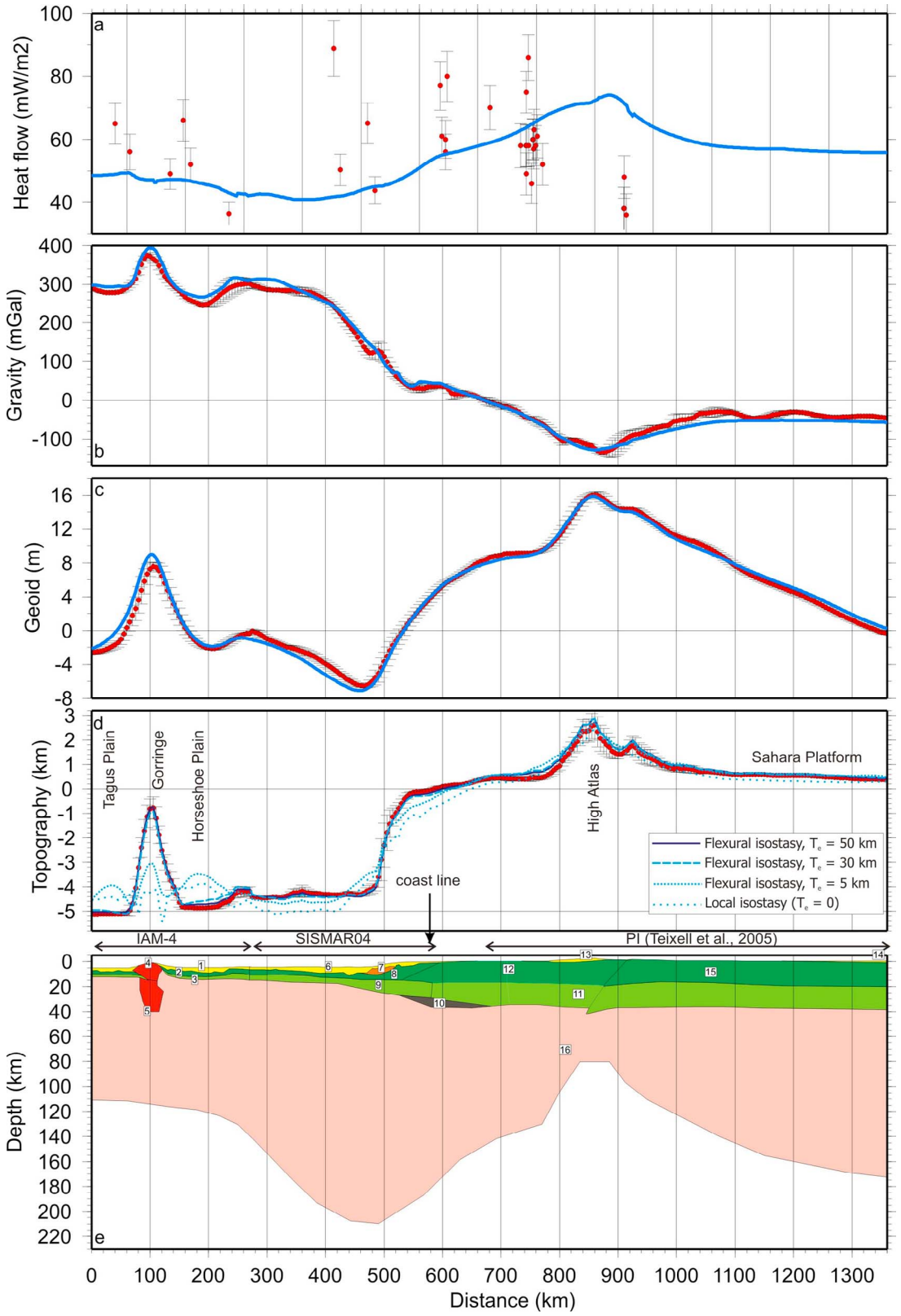

Figure 3. Model results (blue lines) and measured data with the standard deviation indicating lateral variability of data projected into the profile from a strip of 25 km half width (red dots and vertical bars): (a) surface heat flow projected band 100 km and ±10% uncertainty, (b) Bouguer anomaly, (c) Geoid, (d) elevation, and (e) lithosphere structure. Line patterns in Figure 3d indicate different elastic thickness values used to isostatically compensate the lithospheric structure shown in Figure 3e. Numbers in Figure 3e represent the different materials described in Table 1.

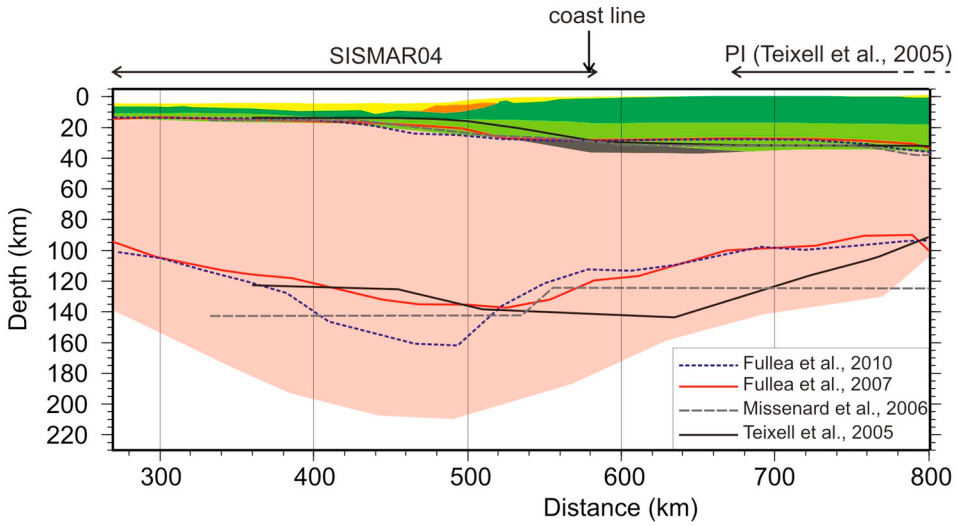

Figure 4. Detail of the lithosphere structure on the margin resulting from our model and Moho and LAB depths from previous studies [*Teixell et al.*, 2005; *Missenard et al.*, 2006; *Fullea et al.*, 2007, 2010]. Different colors represent the same materials as those from Figure 3 and described in Table 1.

and values are summarized in Table 1. Along the SE segment of the transect (from 670 to 1360 km; see Figure 3e) we have used the crustal structure proposed by *Teixell et al.* [2005], modified to introduce a less dense and slightly thicker lower crust to be consistent with the density values proposed by *Contrucci et al.* [2004] beneath the margin (Figure 3e and Table 1). The crust-mantle boundary lies at a depth of 35–38 km reaching a maximum of 40 km beneath the Atlas Mountains.

[7] Along the whole profile we have used a common density value of 2900 kg m^{-3} for the lower crustal layer disregarding its continental, transitional or oceanic affinity, according to the values used in previous works and owing to the lack of reliable data to discriminate the different domains. Thermal conductivities have been ascribed according to previous works and radiogenic heat production according to a recent global compilation by *Vilà et al.* [2010] (Table 1).

[8] An outstanding feature of the NW Moroccan margin is the presence of a high-velocity/high-density lower crustal layer imaged by the SISMAR04 profile beneath the continental platform and mainland. This 8 km thick layer is characterized by Vp of 7.0–7.4 km s^{-1} and a derived density of 3100 kg m^{-3} [*Contrucci et al.*, 2004]. The question is whether this layer is a characteristic of the Hercynian Moroccan lower crust and continues underneath the Atlas Mountains or, alternatively, it is related to rifting and further continental breakup and therefore limited to the margin. Line SISMAR04 is located just north of the northern termination (~35°N) of the West African coast magnetic anomaly (WACMA; see Figure 1), which has been interpreted to be conjugate to the East Coast Magnetic Anomaly (ECMA) located off the shore of eastern North America [*Sahabi et al.*, 2004]. These magnetic anomalies have been related to magmatic rifting between NW Africa and eastern North America

Table 1. Physical Parameters of the Different Bodies Used in the Modeling[a]

Description	ρ (kg m^{-3})	K (W/(K m^{-1}))	H (μW m^{-3})
Ocean sediment	2200–2460	2.0	1.6
Ocean upper crust	2600	2.5	0.5
Ocean lower crust	2900	2.5	0.3
Upper Gorringe (z < 14 km)	2840–3170	2.77	0.03
Deeper Gorringe (z > 14 km)	3180–3290	3.1	0.03
Margin sediment	2180–2540	2.0	1.6
Block margin sediment	2500	2.0	1.6
Margin upper crust	2650	2.5	1.5
Margin lower crust	2900	2.5	0.3
Denser lower crust layer	3100	2.2	0.2
Continent lower crust	2900	2.2	0.2
Hercynia upper crust	2750	3.0	1.6
Atlas sediments	2600	2.4	1.0
Tertiary sediments (Sahara)	2600	2.5	1.4
Sahara upper crust	2750	3.0	1.4
Lithospheric mantle	$3200 \times [1–3.5 \times 10^{-5}\ (T - 1350°C)]$	3.4	0.02

[a]Variables are as follows: ρ, density, which can vary in depth; K, thermal conductivity; H, radiogenic heat production; and z, depth. The density of the lithospheric mantle is temperature-dependent $T(z)$, $\rho_m = \rho_a[1–\alpha(T(z) - T_a)]$, where ρ_a is the density of the asthenosphere (3200 kg m^{-3}), α is the thermal expansion coefficient (3.5×10^{-5} 1/°C), and T_a is the temperature of the asthenosphere (1350°C). Seawater density ρ_w = 1031 kg m^{-3}.

occurring in Triassic-Early Jurassic times [*Labails et al.*, 2009]. Further south, at ~23°N, seismic refraction profiles exhibit a high-velocity (up to 7.25 km s^{-1}) lower crust, which has been interpreted as evidence of modification of the original lower crust by magmatic intrusions into the original crust during the rifting process [*Klingelhoefer et al.*, 2009]. Our profile is located at the northern end of the WACMA where magmatism was less intense than further south as suggested by the lack of seaward dipping reflectors, which are typical of more robust volcanic margins. Therefore, we interpret that the imaged high-velocity lower crust consists of rift-related magmatic underplating and is then restricted to the margin.

4. Modeling Results and Lithosphere Structure

[9] Calculated and measured geophysical observables are compared in Figure 3. Owing to its scarcity, surface heat flow data have been projected onto the profile from a strip of 100 km half width, and we have associated an uncertainty of ±10% to the measured heat flow values. The observed Bouguer and geoid anomalies and elevation gridded data have been projected onto the profile from a strip of 25 km half width, the error bars indicating the standard deviation associated with the lateral variability of each observable.

[10] The forward modeling approach we use assume that the density of the lithospheric mantle is only temperature dependent and that the density of the asthenosphere is constant everywhere [*Zeyen and Fernàndez*, 1994]. Lithosphere rigidity is accounted for when calculating elevation under regional isostasy. Vertical loads relevant to flexure are computed from the lateral changes in lithostatic pressure resulting from the lithospheric structure derived from potential fields (for a detailed explanation, see *Jiménez-Munt et al.* [2010]). Figure 3d shows the lithostatic topography obtained from four different elastic thicknesses (T_e) assumed to be constant along the profile: 0 km (local isostasy), 5 km (weak), 30 km (strong, corresponding to oceanic lithosphere ~140 Ma), and 50 km (rigid lithosphere). The results on Figure 3d suggest that the bulk of the Gorringe Bank topography cannot be sustained by a weak lithosphere of $T_e \approx 0$ (local isostasy) or $T_e \approx 5$ km and values larger than 25–30 km are required to explain its topography [*Jiménez-Munt et al.*, 2010]. In contrast, the high topography in the Atlas Mountains can be sustained by a weak lithosphere ($T_e \approx$ 5 km), as suggested in admittance studies [*Hartley et al.*, 1996; *Pérez-Gussinyé et al.*, 2009], and is in accordance with a hot and thin lithosphere.

[11] Under these conditions, and with the mentioned constraints on the crustal structure, our best fitting model (Figure 3) shows a very good agreement with gravity, geoid and elevation data. Short-wavelength misfits are probably related to the oversimplified upper crustal structure used in the model. The match with surface heat flow data is clearly worse and perturbations related to deep-seated transient effects and/or groundwater circulation owing to the rough topography cannot be ruled out. Nevertheless, the calculated background heat flows in the Proterozoic Sahara Platform (~57 mW m^{-2}) and the 155 Myr old oceanic domain (~49 mW m^{-2}) are compatible with global reported values in similar tectonothermal regions [e.g., *Pollack et al.*, 1993; *Michaut et al.*, 2009; *Jaupart and Mareschal*, 2011]. The obtained lithospheric thickness along the modeled profile is characterized by large variations (Figure 3e). The LAB lies at 110–120 km depth beneath the oceanic domain around the Gorringe Bank and dips to more than 200 km under the continental slope and the adjacent deep and thick sedimentary basin, where the lithospheric mantle roughly duplicates its thickness. Further to the SE, from the continental slope to the Atlas Mountains where the lithospheric mantle thins by more than 130 km, the LAB shallows to ~80 km depth. Toward the Sahara Platform, the lithospheric mantle thickens progressively, and the LAB reaches values of 170 km depth at the SE tip of the profile as expected for Proterozoic lithospheres [e.g., *Poudjom-Djomani et al.*, 2001].

[12] The results obtained in the deep oceanic domains are coincident with those obtained by *Jiménez-Munt et al.* [2010] in the Gorringe Bank region. Beneath the Atlas and the Sahara Platform our values do not differ substantially from those obtained by *Fullea et al.* [2010], who used a 3-D-integrated petrological-geophysical approach, and from the various 2-D transects focused on the Atlas [e.g., *Zeyen et al.*, 2005; *Teixell et al.*, 2005; *Missenard et al.*, 2006]. However, the lithospheric mantle thickening obtained beneath the NW Moroccan margin with a LAB depth of ~210 km exceeds by some tens of kilometers the previously proposed values of 135–165 km [e.g., *Teixell et al.*, 2005; *Missenard et al.*, 2006; *Fullea et al.*, 2007, 2010]. The reasons for this discrepancy are discussed in section 5. However, it is worth noting that reasonable variations in the density values and/or the geometry of the crustal layers do not qualitatively modify the obtained results when simultaneous fitting of all the observables is imposed.

[13] Despite the density values used by *Contrucci et al.* [2004] obtained from empirical velocity-density relationships, the adopted value of 2900 kg m^{-3} for the lower crust based on *Christensen and Mooney*'s [1995] study may seem too low. Therefore, we run a model by setting the lower crustal density to 2950 kg m^{-3} and modifying the thickness of the lower crust beneath the continental section using the values proposed by *Teixell et al.* [2005]. The results show no noticeable differences with the model shown in Figure 3 (2900 kg m^{-3}) owing to the roughly horizontal geometry of the lower crust along the profile.

[14] We also checked how the lithospheric mantle thickening beneath the margin affects the fitting of the model by imposing, according to the mentioned previous works, a LAB depth of 140 km in this region. The results show a regional misfit of more than 50 mGal in the Bouguer anomaly and >15 m in the geoid height anomaly, then supporting the need of a deep LAB in this part of the Moroccan margin.

5. Discussion

5.1. Lithospheric Structure

[15] The most outstanding result of the present study is the lithospheric mantle density anomaly beneath the Moroccan margin, which is explained by a prominent mantle thickening with a LAB depth exceeding 200 km. At crustal levels, this thickening coincides with the presence of a deep sedimentary basin adjacent to the continental slope and a gentle crustal thinning related to the passive extension of the margin. From a modeling viewpoint, mantle thickening is required to make compatible the observed elevation, Bouguer anomaly and

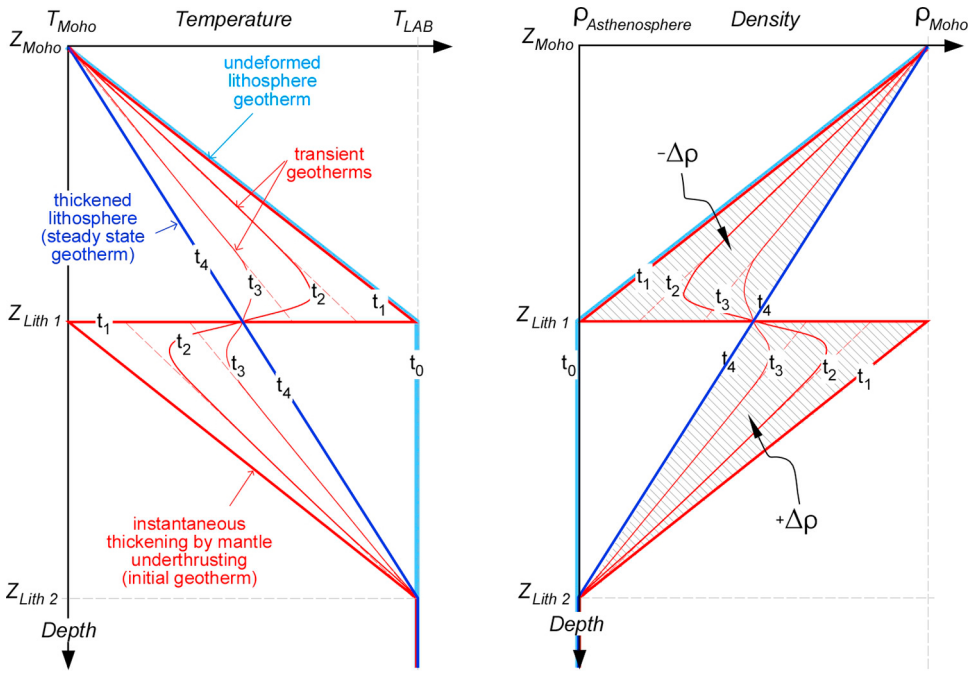

Figure 5. (a) Sketch showing the steady state geotherms for a lithosphere before and after being thickened (light and dark blue lines) and the corresponding transient geotherms (red lines) resulting from the duplication of the lithospheric mantle by underthrusting. (b) Density distribution within the lithospheric mantle as resulting from the geotherms depicted in Figure 5a. Any geotherm corresponding to mantle underthrusting presents a negative density anomaly on the upper plate ($-\Delta\rho$) relative to the steady state geotherm that is balanced with a positive anomaly ($+\Delta\rho$) on the lower plate.

geoid height with the crustal and density structure inferred from the SISMAR04 seismic experiment. Figure 4 compares our results with the lithospheric structure obtained by previous works [*Teixell et al.*, 2005; *Missenard et al.*, 2006; *Fullea et al.*, 2007, 2010] along profiles running very close to ours. It must be noted, however, that these works were not constrained by seismic data across the margin because of their different goals. The obtained results show an incipient lithospheric thickening beneath the Moroccan margin with a maximum LAB depth of 135–165 km, in contrast to the ~210 km proposed in our study. The reason for this discrepancy is twofold. On one side, the model by *Teixell et al.* [2005] shows a similar crustal thinning from the Moroccan Meseta to the abyssal basin but considers a ~10 km thinner crust than imaged by the SISMAR04 survey adopted here. On the other side, the three other previous models [*Missenard et al.*, 2006; *Fullea et al.*, 2007, 2010] use a crustal thickness along the continental slope similar to SISMAR04 but 6–10 km thinner in the Moroccan Meseta, which modifies notoriously the crustal thinning geometry of the margin. In this sense, the presence of the high-velocity/high-density lower crustal layer substituting mantle material has the effect of displacing the LAB downward beneath the proximal margin and the shoreline (560–600 km in horizontal distance; see Figure 4). The thick sedimentary infill and the broad region of crustal stretching [*Klingelhoefer et al.*, 2009] produce a shallow negative density anomaly requiring a deep-seated positive anomaly to fit the geoid height and the deep bathymetry measured in the margin. Finally, differences in the refinement of the upper middle crustal structure and density distribution between the proposed models are also responsible for the encountered discrepancies.

[16] A major limitation is that our numerical approach assumes thermal steady state and conductive heat transfer and then it is not sensitive to mantle flow and/or thermal recovery related to ongoing mantle deformation. The presented results are constrained by the simultaneous fitting of a set of "instantaneous" density-dependent observables such as gravity, geoid and elevation, and then results must be considered as a snapshot of the present-day density distribution related to active tectonic processes. The average mantle density down to 200 km is required to be ~30 kg m^{-3} higher beneath the NW Moroccan margin relative to the surrounding regions. A transient thermal model could improve the calculated temperature and density distribution, but the vertically averaged density anomaly must remain similar to yield similar topography and potential fields. An upper bound on the resulting mass anomaly can be calculated by considering that lithospheric thickening is produced by mantle underthrusting as it is discussed in section 5.3. Underthrusting brings the cold upper surface of the underthrust lithosphere down into the middle to low lithosphere producing a thermal and density inversion. Figure 5 shows the temperature and associated density distributions assuming that underthrusting is instantaneous and after several time intervals during which conductive thermal recovery takes place. The resulting geotherms and depth-density profiles show a null net mass anomaly relative to the steady state. This implies that elevation, calculated under local isostasy, will be exactly the same regardless steady or transient thermal state. The Bouguer

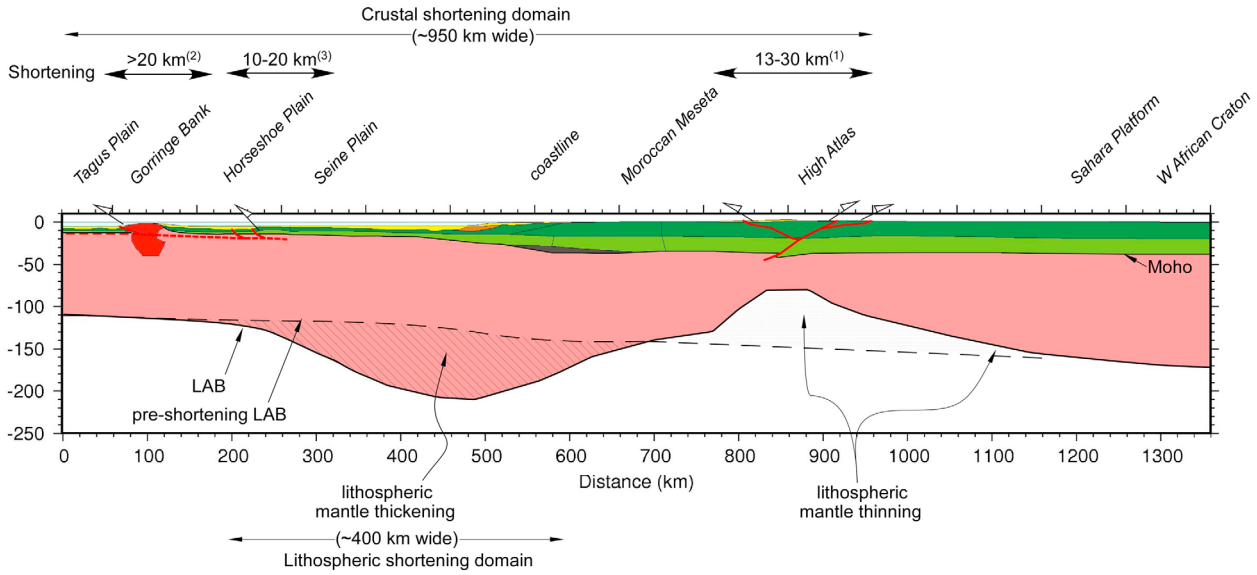

Figure 6. Schematic lithospheric cross section showing the crustal and lithospheric mantle shortening domains. Black dashed line shows the assumed preshortening LAB depth. Crustal shortening references are as follows: 1, *Teixell et al.* [2003]; 2, *Galindo-Zaldívar et al.* [2003] and *Jiménez-Munt et al.* [2010]; and 3, *Zitellini et al.* [2009].

anomaly will be very similar in both cases because of the high depth and the weakness of the density contrast. However, the geoid anomaly can be affected notoriously since it depends on the dipole moment of the density distribution and therefore on the magnitude of the density contrast but also on the vertical distance of the mass dipole.

[17] A rough estimate of the differences in the calculated geoid anomaly corresponding to steady and transient thermal states can be done by assuming the 1-D approach by *Turcotte and Schubert* [2002]. According to this, the geoid difference ΔN is given by

$$\Delta N = -\frac{2\,\pi\,G}{g}\int_{z_m}^{z_2}\Delta\rho(z)z\,dz = -\frac{2\,\pi\,G}{g}\left[\int_{z_m}^{z_1}\left(\frac{\rho_m-\rho_a}{2}\right)\left(\frac{z-Z_m}{Z_1-Z_m}\right)z\,dz + \int_{z_1}^{z_2}\left(\frac{\rho_m-\rho_a}{2}\right)\left(\frac{z-Z_2}{Z_2-Z_1}\right)z\,dz\right]$$

where z is depth measured downward; Z_m the Moho depth, Z_1 and Z_2 are the LAB before and after underthrusting, respectively (see Figure 5); ρ_m and ρ_a are the densities of the lithosphere-mantle at Moho and LAB depths, respectively; g is gravimetric attraction at Earth's surface (9.81 m s^{-2}); and G is universal gravity constant (6.67 × 10^{-11} m^3 kg^{-1} s^{-2}). Substituting the corresponding values (ρ_m = 3300 kg m^{-3}, ρ_a = 3200 kg m^{-3}, Z_m = 25 km, Z_1 = 115 km, Z_2 = 205 km), we find that the geoid difference is <6 m. This huge difference is the uppermost bound since it implies that underthrusting is instantaneous and very recent. If we consider that temperature is partly recovered by thermal conduction, then the geoid difference decreases linearly with the density anomaly resulting in values of about 4 and 2 m for temperatures corresponding to times t_2 and t_3, respectively (Figure 5). Then transient effects introduce additional uncertainties in defining the lithosphere-asthenosphere geometry. A more precise temperature distribution would require a detailed knowledge of the evolution of the margin and additional constraints as the tectonic subsidence through time, which is beyond the scope of this study.

[18] Another limitation is that lateral variations in either the lithospheric mantle density related to compositional differences between the oceanic and the continental domains or in asthenosphere density induced by variations in the sublithospheric thermal gradient are not considered. The required mantle density contrast of 30 kg m^{-3} cannot be explained by compositional differences since the density of a 150 Myr old oceanic lithosphere mantle exceeds as much as 10 kg m^{-3} the average density of a Phanerozoic continental mantle [e.g., *Afonso et al.*, 2008; *Fullea et al.*, 2010]. Density variations within the asthenosphere could be related to either the LAB topography or to vertical flow. In the first case, the lateral differences in the sublithospheric thermal gradient are in the range of 0.2–0.3 K km^{-1}. In the second case, the lateral temperature variations related to small-scale convection, or even full convection in the upper mantle, are of few tens of degrees especially when adiabatic heating is taken into account [e.g., *Zlotnik et al.*, 2008a, 2008b]. In both cases, the temperature variations are too low to produce a noticeable effect on the average density of the asthenosphere.

5.2. Crust-Mantle Decoupling

[19] Figure 6 shows our geological interpretation of the present-day lithospheric structure along the modeled profile. The large variations in the lithospheric mantle thickness contrast with the more homogeneous crustal structure, whose main variations are related to the Gorringe thrusting structure, the intracontinental fold belt of the Atlas Mountains, and the rifted passive margin (Figure 6). These differences in the crust

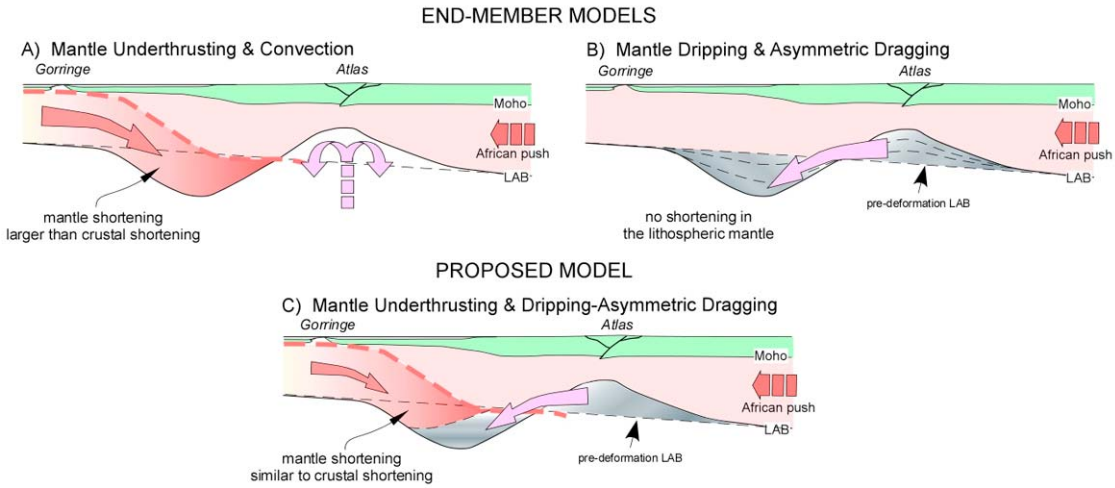

Figure 7. Cartoon showing the end-member models to explain lithosphere mantle thickening and adjacent thinning: (a) mantle underthrusting related to plate convergence and thermal erosion produced by convection or mantle plume and (b) lateral displacement of mantle material related to mantle dripping and dragging. (c) Preferred model for the NW Moroccan margin: underthrusting related to similar amount of crustal shortening plus lateral displacement of all the material missing beneath the Atlas due to dripping and lateral dragging.

and lithosphere mantle geometries indicate that the Africa-Eurasia convergence in this segment of the plate boundary is dominated by crust-mantle strain partitioning. Decoupling between crust and mantle is also evidenced by the contrasting widths of the regions over which crust and mantle shortening are accommodated (Figure 6). Whereas crustal shortening is accommodated sparsely over a ~950 km wide region, most of the lithospheric mantle shortening is absorbed on the Moroccan margin over a ~400 km wide region.

[20] Crustal restoration analyses performed in the High Atlas indicate that deformation decreases along strike from east to west from 24% to 15% implying shortening values between 13 and 30 km [*Teixell et al.*, 2003]. In the Gorringe Bank, estimates of crustal shortening yielded minimum values of 20 km [*Galindo-Zaldívar et al.*, 2003; *Jiménez-Munt et al.*, 2010]. If we consider 10–20 km of additional shortening related to the Horseshoe-Coral Patch Seamount thrust and the anticlines south of the Coral Patch Ridge [*Zitellini et al.*, 2009], then the total crustal shortening could range between 40 and 60 km. The anti-Atlas Mountains also record a shortening of 18–25 km [e.g., *Helg et al.*, 2004; *Burkhard et al.*, 2006], but deformation occurred in Late Carboniferous–Early Permian times and is not relevant to our analysis. At subcrustal levels, the prominent lithospheric thickness variations along the profile suggest higher values of shortening at mantle scale and/or the participation of different processes.

5.3. Geodynamic Mechanisms of Lithosphere Deformation

[21] The results implying a marked difference in crustal and mantle shortening pose a severe problem in interpreting the geodynamic evolution of the region. The measured crustal shortening is lower than that predicted by relative plate movements. A shortening of ~150 km would be in good agreement with the displacement of Africa relative to Eurasia during the last 55 Myr as derived from plate kinematic reconstructions [*Rosenbaum et al.*, 2002]. But this amount of convergence, when applied to the crust, implies ~16% of average crustal shortening distributed over a region 950 km wide, which apparently is not supported by geological observations. Hence, tectonic shortening must be accommodated at crustal levels either farther NW of the Gorringe Bank region into the Iberian-Atlantic oceanic domains or off the strike of the profile, or a combination of both. Part of this accommodation is presently observed in the Horseshoe Plain and the Gulf of Cadiz accretionary wedge where a WNW–ESE lineament of strike-slip faults (SWIM lineament) [*Zitellini et al.*, 2009] has been proposed as the modern (2 Ma) plate boundary.

[22] Depending on whether the mantle thickening beneath the continental margin is linked or not to the adjacent mantle thinning beneath the Atlas, we can propose two end-member models to explain the inferred lithosphere geometry (Figure 7). In the first end-member case (Figure 7a), thickening is entirely produced by mantle underthrusting related to tectonic convergence, whereas sublithospheric mantle activity (convection or "baby plume") is responsible for the adjacent mantle thinning. The action of these two mechanisms has been recently proposed by *Fullea et al.* [2010], who analyzed the geodynamic implications of the modeled 3-D crustal and lithospheric structure in the Atlantic-Mediterranean transition region. Fullea et al. separate the mantle thickening imaged in the NW Moroccan margin produced by the slow and protracted convergence between Africa and Eurasia from that affecting the Gibraltar Arc, which is related to subduction/delamination of the westernmost Alpine-Tethys oceanic domain. In agreement with previous work [e.g., *Hoernle et al.*, 1995; *Zeyen et al.*, 2005], Fullea et al. propose small-scale convection or baby plume activity as the mechanism

causing mantle thinning beneath the Atlas. As a second end-member case (Figure 7b), we propose a single mechanism consisting of gravitational instability leading to thickening by mantle dripping and thinning by asymmetric lateral dragging of the adjacent mantle. This mechanism has been proposed for the Southern Carpathians by *Lorinczi and Houseman* [2009], who present a 3-D numerical model of an asymmetric Rayleigh-Taylor instability. Despite the many differences that characterize both settings, the results obtained in the Southern Carpathians in terms of lithospheric thickness and characteristic time for a non-Newtonian mantle with stress exponent $n = 3$ [see *Lorinczi and Houseman*, 2009, Figure 8] resemble much that figured in the NW Moroccan margin. *Houseman et al.* [2000] examined the Rayleigh-Taylor instability occurring beneath a convergent zone, and they established that mantle downwelling on the margins of a convergent belt is a possible outcome when the crustal layer is relatively weak (also proposed by *Valera et al.* [2011]), and the rate of forced convergence is relatively low. The Moroccan margin could be an example of this type of process, where the convergence rate is low and a weak crustal layer would be in agreement with the crust-mantle decoupling observed. However, none of these end-member mechanisms can explain by themselves the inferred mantle geometry since underthrusting would require a shortening larger than the total relative plate motion between Africa and Eurasia, whereas dripping and dragging is not balancing the thickening beneath the margin and the thinning beneath the Atlas.

[23] A plausible model (Figure 7c) considers that all the material missing beneath the Atlas was dragged by a mantle drip beneath the margin probably triggered by mantle underthrusting. In this case, an amount of in-plane convergence similar to the estimated crustal shortening (40–60 km) suffices to explain the inferred mantle geometry and overcomes the discrepancy between crust and mantle shortening estimates.

[24] According to the 3-D lithospheric model by *Fullea et al.* [2010], mantle thickening vanishes to the SW along the African margin. Recently acquired DAKHLA seismic reflection and wide-angle data [*Klingelhoefer et al.*, 2009] support this idea showing that the crustal structure of the SW and NW Moroccan margins differs noticeably. The undeformed crust in the SW Moroccan margin appears to be ~8 km thinner, and the region affected by crustal stretching appears to be ~50 km narrower than in the northern part of the margin. The thinner crust together with the geoid signature supports the absence of mantle underthrusting in the SW margin in agreement to the progressive change of the relative Africa-Eurasia motion along the Moroccan margin owing to the proximity of the rotation pole [*Argus et al.*, 1989]. Active underthrusting of oceanic crust has been also proposed by *Déverchère et al.* [2005] in the Algerian-Mediterranean margin where the convergence of Africa has a higher perpendicular component.

6. Concluding Remarks

[25] The combination of wide-angle and seismic reflection data with integrated numerical modeling of the geopotential, lithostatic and thermal regime of the lithosphere has allowed us to image the lithospheric structure across the NW Moroccan margin along a profile striking from the Gorringe Bank to the Sahara Platform. Our lithosphere structure along the margin, which is based on its density distribution, differs noticeably from previous studies owing to the ~10 km thicker crust modeled by *Contrucci et al.* [2004]. The main concluding remarks extracted from this study are as follows:

[26] 1. The inferred positive mantle density anomaly beneath the NW Moroccan margin is explained by a prominent lithospheric mantle thickening coinciding with the region of major crustal stretching and sedimentary infill. The LAB could reach a depth of >200 km exceeding previous estimations by some tens of km.

[27] 2. The strong differences in the derived crustal and lithospheric mantle structures and the width over which the Africa-Eurasia convergence is accommodated reveal a significant strain partitioning and decoupling between the crust and the lithospheric mantle.

[28] 3. According to geological observations, crustal shortening is concentrated on the Gorringe Bank, the Atlas Mountains and the Horseshoe Coral Patch region, amounting to 40–60 km. This amount represents ~1/3 of the total relative plate motion between Africa and Eurasia during the last 55 Myr, and thus, part of the convergence must be accommodated farther NW of the Gorringe Bank and/or off the strike of the profile.

[29] 4. A model in which mantle underthrusting accommodates 50–60 km of convergence combined with mantle dripping and lateral dragging of the whole volume involved in the thinned lithospheric mantle beneath the Atlas region makes the estimated crustal and lithospheric shortening and the imaged lithospheric structure compatible.

[30] **Acknowledgments.** This research was funded partly by Projects TopoMed (CGL2008-03474-E/BTE), ESF-Eurocores 07-TOPOEUROPE-FP006, TopoAtlas (CGL2006-05493/BTE), SISAT (CGL2008-01124-E/BTE), ATIZA (CGL2009-09662-BTE), and Consolider-Ingenio 2010 Topo-Iberia (CSD2006-00041). Constructive reviews from Greg Houseman and an anonymous reviewer, as well as the advice of the Associate Editor, helped us improve the final version.

References

Afonso, J. C., M. Fernàndez, G. Ranalli, W. L. Griffin, and J. A. D. Connolly (2008), Integrated geophysical-petrological modeling of the lithosphere and sublithospheric upper mantle: Methodology and applications, *Geochem. Geophys. Geosyst.*, *9*, Q05008, doi:10.1029/2007GC001834.

Argus, D. F., R. G. Gordon, C. DeMets, and S. Stein (1989), Closure of the Africa-Eurasia-North America plate motion circuit and tectonics of the Gloria fault, *J. Geophys. Res.*, *94*, 5585–5602, doi:10.1029/JB094iB05p05585.

Banda, E., M. Torne, and the IAM Group (1995), Iberian Atlantic Margins Group investigates deep structure of ocean margins, *Eos Trans. AGU*, *76*(3), 25.

Bijwaard, H., and W. Spakman (2000), Non-linear global *P* wave tomography by iterated linearized inversion, *Geophys. J. Int.*, *141*, 71–82, doi:10.1046/j.1365-246X.2000.00053.x.

Buforn, E., A. Udías, and M. A. Colombás (1988), Seismicity, source mechanisms and tectonics of the Azores-Gibraltar plate boundary, *Tectonophysics*, *152*, 89–118, doi:10.1016/0040-1951(88)90031-5.

Burkhard, M., S. Caritg, U. Helg, C. Robert-Charrue, and A. Soulaimani (2006), Tectonics of the anti-Atlas of Morocco, *C. R. Geosci.*, *338*, 11–24, doi:10.1016/j.crte.2005.11.012.

Calais, E., C. DeMets, and J. M. Nocquet (2003), Evidence for a post-3.16-Ma change in Nubia–Eurasia–North America plate motions?, *Earth Planet. Sci. Lett.*, *216*, 81–92, doi:10.1016/S0012-821X(03)00482-5.

Calvert, A., E. Sandvol, D. Seber, M. Barazangi, S. Roecker, T. Mourabit, F. Vidal, G. Alguacil, and N. Jabour (2000), Geodynamic evolution of

the lithosphere and upper mantle beneath the Alboran region of the western Mediterranean: Constraints from travel time tomography, *J. Geophys. Res.*, *105*, 10,871–10,898, doi:10.1029/2000JB900024.

Christensen, N. I., and W. D. Mooney (1995), Seismic velocity structure and composition of the continental crust: A global view, *J. Geophys. Res.*, *100*, 9761–9788, doi:10.1029/95JB00259.

Contrucci, I., F. Klingelhoefer, J. Perrot, R. Bartolome, M.-A. Gutscher, M. Sahabi, J. Malod, and J.-P. Rehault (2004), The crustal structure of the NW Moroccan continental margin from wide-angle and reflection seismic data, *Geophys. J. Int.*, *159*, 117–128, doi:10.1111/j.1365-246X.2004.02391.x.

Déverchère, J., et al. (2005), Active thrust faulting offshore Boumerdes, Algeria, and its relations to the 2003 Mw 6.9 earthquake, *Geophys. Res. Lett.*, *32*, L04311, doi:10.1029/2004GL021646.

Fernandes, R. M. S., J. M. Miranda, B. M. L. Meijninger, M. S. Bos, R. Noomen, L. Bastos, B. A. C. Ambrosius, and R. E. M. Riva (2007), Surface velocity field of the Ibero-Maghrebian segment of the Eurasia-Nubia plate boundary, *Geophys. J. Int.*, *169*, 315–324, doi:10.1111/j.1365-246X.2006.03252.x.

Fernàndez, M., I. Marzán, A. Correia, and E. Ramalho (1998), Heat flow, heat production, and lithospheric thermal regime in the Iberian Peninsula, *Tectonophysics*, *291*, 29–53, doi:10.1016/S0040-1951(98)00029-8.

Fullea, J., M. Fernàndez, H. Zeyen, and J. Vergés (2007), A rapid method to map the crustal and lithospheric thickness using elevation, geoid anomaly and thermal analysis: Application to the Gibraltar Arc System, Atlas Mountains and adjacent zones, *Tectonophysics*, *430*, 97–117, doi:10.1016/j.tecto.2006.11.003.

Fullea, J., M. Fernàndez, and H. Zeyen (2008), FA2BOUG—A FORTRAN 90 code to compute Bouguer gravity anomalies from gridded free air anomalies: Application to the Atlantic-Mediterranean transition zone, *Comput. Geosci.*, *34*, 1665–1681, doi:10.1016/j.cageo.2008.02.018.

Fullea, J., M. Fernàndez, J. C. Afonso, J. Vergés, and H. Zeyen (2010), The structure and evolution of the lithosphere-asthenosphere boundary beneath the Atlantic-Mediterranean Transition Region, *Lithos*, *120*, 74–95, doi:10.1016/j.lithos.2010.03.003.

Galindo-Zaldívar, J., A. Maldonado, and A. A. Schreider (2003), Gorringe Ridge gravity and magnetic anomalies are compatible with thrusting at crustal scale, *Geophys. J. Int.*, *153*, 586–594, doi:10.1046/j.1365-246X.2003.01922.x.

Grevemeyer, I., N. Kaul, and A. Kopf (2009), Heat flow anomalies in the Gulf of Cadiz and off Cape San Vicente, Portugal, *Mar. Pet. Geol.*, *26*, 795–804, doi:10.1016/j.marpetgeo.2008.08.006.

Hartley, R., A. B. Watts, and J. D. Fairhead (1996), Isostasy of Africa, *Earth Planet. Sci. Lett.*, *137*, 1–18, doi:10.1016/0012-821X(95)00185-F.

Helg, U., M. Burkhard, S. Caritg, and C. Robert-Charrue (2004), Folding and inversion tectonics in the anti-Atlas of Morocco, *Tectonics*, *23*, TC4006, doi:10.1029/2003TC001576.

Hildenbrand, T., R. Kucks, M. Hamouda, and A. Bellot (1988), Bouguer gravity map and related filtered anomaly maps of Morocco, *U.S. Geol. Surv. Open File Rep.*, *88-517*, 15 pp.

Hoernle, K., Y.-S. Zhang, and D. Graham (1995), Seismic and geochemical evidence for large-scale mantle upwelling beneath the eastern Atlantic and western and central Europe, *Nature*, *374*, 34–39, doi:10.1038/374034a0.

Houseman, G. A., E. A. Neil, and M. D. Kohler (2000), Lithospheric instability beneath the Transverse Ranges of California, *J. Geophys. Res.*, *105*, 16,237–16,250, doi:10.1029/2000JB900118.

Jaffal, M., F. Klingelhoefer, L. Matias, F. Teiseira, and M. Amrhar (2009), Crustal structure of the NW Moroccan margin from deep seismic data (SISMAR cruise), *C. R. Geosci.*, *341*, 495–503, doi:10.1016/j.crte.2009.04.003.

Jaupart, C., and J. C. Mareschal (2011), *Heat Generation and Transport in the Earth*, 465 pp., Cambridge Univ. Press, Cambridge, U.K.

Jiménez-Munt, I., and A. Negredo (2003), Neotectonic modelling of the western part of the Africa–Eurasia plate boundary: From the Mid-Atlantic Ridge to Algeria, *Earth Planet. Sci. Lett.*, *205*, 257–271, doi:10.1016/S0012-821X(02)01045-2.

Jiménez-Munt, I., M. Fernàndez, M. Torné, and P. Bird (2001), The transition from linear to diffuse plate boundary in the Azores-Gibraltar region: Results from a thin-sheet model, *Earth Planet. Sci. Lett.*, *192*, 175–189, doi:10.1016/S0012-821X(01)00442-3.

Jiménez-Munt, I., M. Fernàndez, J. Vergés, J. C. Afonso, D. Garcia-Castellanos, and F. Fullea (2010), Lithospheric structure of the Gorringe Bank: Insights into its origin and tectonic evolution, *Tectonics*, *29*, TC5019, doi:10.1029/2009TC002458.

Klingelhoefer, F., C. Labails, E. Cosquer, S. Rouzo, L. Géli, D. Aslanian, J.-L. Olivet, M. Sahabi, H. Nouzé, and P. Unternehr (2009), Crustal structure of the SW-Moroccan margin from wide-angle and reflection seismic data (the DAKHLA experiment) part A: Wide-angle seismic models, *Tectonophysics*, *468*, 63–82, doi:10.1016/j.tecto.2008.07.022.

Labails, C., J. L. Olivet, and the Dakhla Study Group (2009), Crustal structure of the SW-Moroccan margin from wide-angle and reflection seismic data (the DAKHLA experiment) part B: The tectonic heritage, *Tectonophysics*, *468*, 83–97, doi:10.1016/j.tecto.2008.08.028.

Lindquist, K. G., K. Engle, D. Stahlke, and E. Price (2004), Global topography and bathymetry grid improves research efforts, *Eos Trans. AGU*, *85*(19), 186, doi:10.1029/2004EO190003.

Lorinczi, P., and G. A. Houseman (2009), Lithospheric gravitational instability beneath the southeast Carpathians, *Tectonophysics*, *474*, 322–336, doi:10.1016/j.tecto.2008.05.024.

Michaut, C., C. Jaupart, and J.-C. Mareschal (2009), Thermal evolution of cratonic roots, *Lithos*, *109*, 47–60, doi:10.1016/j.lithos.2008.05.008.

Missenard, Y., H. Zeyen, D. Frizon de Lamotte, P. Leturmy, C. Petit, M. Sébrier, and O. Saddiqi (2006), Crustal versus asthenospheric origin of relief of the Atlas Mountains of Morocco, *J. Geophys. Res.*, *111*, B03401, doi:10.1029/2005JB003708.

Nocquet, J. M., and E. Calais (2004), Geodetic measurements of crustal deformation in the western Mediterranean and Europe, *Pure Appl. Geophys.*, *161*, 661–681, doi:10.1007/s00024-003-2468-z.

Pavlis, N. K., S. A. Holmes, S. C. Kenyon, and J. K. Factor (2008), An Earth gravitational model to degree 2160, paper presented at EGU 2008, Eur. Geosci. Union, Vienna, 13–18 Apr.

Pérez-Gussinyé, M., M. Metois, M. Fernàndez, J. Vergés, J. Fullea, and A. R. Lowry (2009), Effective elastic thickness of Africa and its relationship to other proxies for lithospheric structure and surface tectonics, *Earth Planet. Sci. Lett.*, *287*, 152–167, doi:10.1016/j.epsl.2009.08.004.

Pollack, H. N., S. J. Hurter, and J. R. Johnson (1993), Heat flow from the Earth's interior analysis of the global data set, *Rev. Geophys.*, *31*, 267–280, doi:10.1029/93RG01249.

Polyak, B. G., et al. (1996), Heat flow in the Alboran Sea, western Mediterranean, *Tectonophysics*, *263*, 191–218, doi:10.1016/0040-1951(95)00178-6.

Poudjom-Djomani, Y. H., S. Y. O'Reilly, W. L. Griffin, and P. Morgan (2001), The density structure of subcontinental lithosphere through time, *Earth Planet. Sci. Lett.*, *184*, 605–621, doi:10.1016/S0012-821X(00)00362-9.

Rimi, A., A. Chalouan, and L. Bahi (1998), Heat flow in the westernmost part of the Alpine Mediterranean system (the Rif, Morocco), *Tectonophysics*, *285*, 135–146, doi:10.1016/S0040-1951(97)00185-6.

Rosenbaum, G., G. S. Lister, and C. Duboz (2002), Relative motions of Africa, Iberia and Europe during Alpine orogeny, *Tectonophysics*, *359*, 117–129, doi:10.1016/S0040-1951(02)00442-0.

Sahabi, M., D. Aslanian, and J.-L. Olivet (2004), A new starting point for the history of the central Atlantic, *C. R. Geosci.*, *336*, 1041–1052, doi:10.1016/j.crte.2004.03.017.

Sandwell, D. T., and W. H. F. Smith (1997), Marine gravity anomalies from GEOSAT and ERS-1 satellite altimetry, *J. Geophys. Res.*, *102*, 10,039–10,054, doi:10.1029/96JB03223.

Sartori, R., L. Torelli, N. Zitellini, D. Peis, and E. Lodolo (1994), Eastern segment of the Azores-Gibraltar line (central-eastern Atlantic): An oceanic plate boundary with diffuse compressional deformation, *Geology*, *22*, 555–558, doi:10.1130/0091-7613(1994)022<0555:ESOTAG>2.3.CO;2.

Teixell, A., M.-L. Arboleya, M. Julivert, and M. Charroud (2003), Tectonic shortening and topography in the central High Atlas (Morocco), *Tectonics*, *22*(5), 1051, doi:10.1029/2002TC001460.

Teixell, A., P. Ayarza, H. Zeyen, M. Fernàndez, and M. L. Arboleya (2005), Effects of mantle upwelling in a compressional setting: The Atlas Mountains of Morocco, *Terra Nova*, *17*, 456–461, doi:10.1111/j.1365-3121.2005.00633.x.

Turcotte, D. L., and G. Schubert (2002), *Geodynamics*, 2nd ed., 445 pp., Cambridge Univ. Press, Cambridge, U.K.

Valera, J. L., A. M. Negredo, and I. Jiménez-Munt (2011), Deep and near-surface consequences of root removal by asymmetric continental delamination, *Tectonophysics*, *502*, 257–265, doi:10.1016/j.tecto.2010.04.002.

Verzhbitsky, E. V., and V. G. Zolotarev (1989), Heat flow and the Eurasian-African plate boundary in the eastern part of the Azores-Gibraltar fracture zone, *J. Geodyn.*, *11*, 267–273, doi:10.1016/0264-3707(89)90009-4.

Vilà, M., M. Fernàndez, and I. Jiménez-Munt (2010), Radiogenic heat production variability of some common lithological groups and its significance to lithospheric thermal modeling, *Tectonophysics*, *490*, 152–164, doi:10.1016/j.tecto.2010.05.003.

Zeyen, H., and M. Fernàndez (1994), Integrated lithospheric modeling combining thermal, gravity, and local isostasy analysis: Application to

the NE Spanish geotransect, *J. Geophys. Res.*, *99*, 18,089–18,102, doi:10.1029/94JB00898.

Zeyen, H., P. Ayarza, M. Fernàndez, and A. Rimi (2005), Lithospheric structure under the western African–European plate boundary: A transect across the Atlas Mountains and the Gulf of Cadiz, *Tectonics*, *24*, TC2001, doi:10.1029/2004TC001639.

Zitellini, N., et al. (2009), The quest for the Africa-Eurasia plate boundary west of the Strait of Gibraltar, *Earth Planet. Sci. Lett.*, *280*, 13–50, doi:10.1016/j.epsl.2008.12.005.

Zlotnik, S., J. C. Afonso, P. Díez, and M. Fernàndez (2008a), Small-scale gravitational instabilities under the oceans: Implications for the evolution of oceanic lithosphere and its expression in geophysical observables, *Philos. Mag.*, *88*, 3197–3217, doi:10.1080/14786430802464248.

Zlotnik, S., M. Fernàndez, P. Díez, and J. Vergés (2008b), Modelling gravitational instabilities: Slab break-off and Raleigh-Taylor diapirism, *Pure Appl. Geophys.*, *165*, 1491–1510, doi:10.1007/s00024-004-0386-9.

J. C. Afonso, GEMOC ARC National Key Centre, Macquarie University, Sydney, NSW 2109, Australia.

M. Fernàndez, D. Garcia-Castellanos, I. Jiménez-Munt, and J. Vergés, Group of Dynamics of the Lithosphere, Institute of Earth Sciences Jaume Almera, CSIC, Sole Sabarís s/n, E-08028 Barcelona, Spain. (ivone@ictja.csic.es)

J. Fullea, Dublin Institute for Advanced Studies, 5 Merrion Square, Dublin 2, Ireland.

M. Pérez-Gussinyé, Department of Earth Sciences, Royal Holloway University of London, Egham TW20 0EX, UK.